Published in final edited form as:
Vet Ophthalmol. 2011 September ; 14(5): 304–312. doi:10.1111/j.1463-5224.2011.00877.x.

Mitomycin C: a promising agent for the treatment of canine corneal scarring

Rangan Gupta[*,†], **Benjamin W. Yarnall**[*,‡], **Elizabeth A. Giuliano**[*,‡], **Jagat R. Kanwar**[§], **Dylan G. Buss**[*,‡], and **Rajiv R. Mohan**[*,†,‡]

[*]Harry S. Truman Veterans Memorial Hospital, Columbia, MO, USA

[†]Mason Eye Institute, School of Medicine, University of Missouri, Columbia, MO, USA

[‡]College of Veterinary Medicine, University of Missouri, Columbia, MO, USA

[§]Laboratory of Immunology and Molecular Biomedical Research, Centre for Biotechnology and Interdisciplinary Biosciences (BioDeakin), Institute for Technology and Research Innovation, Deakin University, Geelong, Vic. 3217, Australia

Abstract

Objective—To evaluate the safety and efficacy of mitomycin C (MMC) in prevention of canine corneal scarring.

Methods—With an *in vitro* approach using healthy canine corneas, cultures of primary canine corneal fibroblasts or myofibroblasts were generated. Primary canine corneal fibroblasts were obtained by growing corneal buttons in minimal essential medium supplemented with 10% fetal bovine serum. Canine corneal myofibroblasts were produced by growing cultures in serum-free medium containing transforming growth factor β1 (1 ng/mL). Trypan blue assay and phase-contrast microscopy were used to evaluate the toxicity of three doses of MMC (0.002%, 0.02% and 0.04%). Real-time PCR, immunoblot, and immunocytochemistry techniques were used to determine MMC efficacy to inhibit markers of canine corneal scarring.

Results—A single 2-min treatment of 0.02% or less MMC did not alter canine corneal fibroblast or keratocyte phenotype, viability, or growth. The 0.02% dose substantially reduced myofibroblast formation (up to 67%; $P < 0.001$), as measured by the change in RNA and protein expression of fibrosis biomarkers (α-smooth muscle actin and F-actin).

Conclusion—This *in vitro* study suggests that a single 2-min 0.02% MMC treatment to the canine corneal keratocytes is safe and may be useful in decreasing canine corneal fibrous metaplasia. *In vivo* studies are warranted.

Keywords

canine; cornea; fibroblasts; fibrosis; mitomycin C

INTRODUCTION

Corneal fibrosis results in significant canine vision impairment, adversely affecting the service dog (e.g. guide dogs for the blind) and canine pet populations worldwide. Corneal wounds resulting from trauma, disease, or surgery are common ocular causes for dogs to be

Address communications to: R. R. Mohan, Tel.: (573) 884-1449, Fax: (573) 814-6551, mohanr@health.missouri.edu.

seen by veterinarians in both general and specialty practices worldwide. Corneal fibrosis (i.e. corneal scarring) is a common sequel to various canine keratopathies and often terminates in significant visual impairment. Vision loss as a result of corneal fibrosis can result in canine behavioral changes and in the case of agility or service dogs, may impair their work performance. Although a fibrotic response is an essential component of normal healing, it can induce significant opacification to the healthy transparent cornea.[1] To date, therapies specifically targeting the treatment of canine corneal fibrosis are limited in veterinary ophthalmology.[1] However, with the ever-expanding field of corneal surface ablations in physician ophthalmology, strategies aimed at reducing corneal fibrosis have become extensively studied.

Corneal insult that results after surface ablation is known to trigger a cascade of physiologic events that may culminate in mild to severe corneal fibrosis. Modern technologies including photorefractive keratectomy (PRK) which involve mechanical removal of the corneal epithelium have demonstrated an up-regulation of various interleukins including IL-1, IL-8, transforming growth factor beta-1 (TGFβ1) as well as monocyte chemo-attractant protein-1 (MCP-1) in corneal epithelium and stroma. IL-1 indirectly contributes to corneal fibrosis by inducing inflammation.[2] On the other hand, TGFβ1 directly activates keratocytes and leads to formation of myofibroblasts as well as subsequent reformation of subepithelial stromal tissue following PRK.[3] Myofibroblasts scatter more light than the undifferentiated fibroblasts or keratocytes, not only from their nuclei, but also from their cell bodies and dendritic processes.[4–6] In addition, myofibroblasts participate in extracellular matrix remodeling, resulting in denser and more disorganized extracellular matrix, with abundant collagen type III and IV formation. Collectively, these changes lead to loss of corneal transparency.[4–7] The intracellular microfilament fibers such as F-actin and alpha smooth muscle actin (αSMA) have a much higher expression in myofibroblasts than keratocytes. These cellular components enable myofibroblasts to contract and close wounds, but also render the cornea less translucent. [8] Over the last two decades mitomycin C (MMC), a genotoxic antibiotic, has been increasingly used in physician ophthalmology for its anti-fibrotic effects as topical adjunctive therapy for corneal disease and surgery.[9] When applied topically, MMC inhibits cell migration and extracellular matrix production.[10] Intra-operative application of MMC has been used prophylactically to prevent corneal haze formation after surface ablation.[11,12] MMC has been shown to reduce corneal haze by inhibiting the expression of αSMA, induction of cellular apoptosis, and blocking differentiation of mature fibroblasts to myofibroblasts.[13–16]

The exact mechanism resulting in the therapeutic effect of MMC is not fully understood. Up-regulation of certain cytokines such as IL-8 and MCP-1 by activation of protein kinases,[17] induction of Fas-mediated apoptosis,[18,19] as well as apoptosis through activation of caspase cascades with mitochondrial dysfunctions have been implicated in MMC-mediated therapeutic effects.[16,19] Currently, clinically tested doses of MMC(≤0.02% for 2 min) are widely used by physician ophthalmologists to prevent corneal haze formation.[12] In veterinary ophthalmology, MMC has been shown to effectively reduce corneal scarring in rabbits *in vivo*[14] and horses *in vitro*.[20] MMC has been used in dogs to treat malignancies; [21,22] however, to our knowledge, no studies have tested its ability to reduce canine corneal fibrosis. The aim of this study was to examine the safety and efficacy of MMC in treating canine corneal scarring using an *in vitro* model.

MATERIALS AND METHODS

Canine stromal fibroblast (CSF) culture

Corneal buttons were aseptically harvested from healthy research dogs undergoing humane euthanasia for reasons unrelated to this study. Slit-lamp biomicroscopy was performed by a

board-certified veterinary ophthalmologist (EAG) prior to euthanasia to ensure that all harvested samples were from dogs free of anterior segment disease. Corneal buttons were washed with minimum essential medium (MEM, Gibco; Invitrogen, Carlsbad, CA, USA) and the epithelium and endothelium was removed by gentle scraping using a #10 Bard Parker scalpel blade (BD, Franklin Lakes, NJ, USA). Corneal stroma was sub-sectioned and placed in tissue culture plates containing Dulbecco's modified Eagle's medium (DMEM, Gibco; Invitrogen) supplemented with 10% fetal bovine serum to obtain CSFs. The CSFs were then incubated in a humidified CO_2 incubator (HERAcell; Thermo Scientific, Asheville, NC, USA) at 37 °C. In approximately 3–10 days, fibroblasts began migrating from the corneal explants. Once the primary culture reached 90% confluence, the corneal explants were manually removed using rat-toothed forceps and discarded. The confluent cells were trypsinized, cellular concentrations calculated using Countess automated cell counter (Invitrogen) and re-plated on 100 mm tissue culture plates. Passages 1–3 of CSFs were used for this experiment. The monocultures of corneal keratocytes, fibroblasts and myofibroblasts were selectively induced from the primary cultures generated from canine corneal explants by altering media or cell seeding conditions. Cell population and phenotype were constantly monitored to detect epithelial or endothelial contamination. Myofibroblast cultures were induced from fibroblasts using serum-free MEM medium containing 1 ng/mL TGFβ1 cell culture conditions.

Cytotoxicity studies

The cytotoxicity of MMC to CSFs was evaluated using phase-contrast microscopy, trypan blue reagent (Invitrogen), and terminal deoxynucleotidyl transferase-mediated dUTP nick end labeling (TUNEL) assays. Microscopy was used to evaluate cellular morphological alterations. Trypan blue assay assessed cellular viability. TUNEL assay detected apoptotic cells in cultures treated with 0.02% MMC. Microscopy investigations utilized a phase-contrast microscope (Leica DMIL; Leica, Wetzlar, Germany) equipped with an imaging system (Leica DFC290; Leica). The CSF cultures treated with various concentrations of MMC were examined and cell morphology was recorded using digital photography.

Trypan blue assay was performed following manufacturer's instructions. Briefly, 60–70% confluent cells were treated with 0.002%, 0.02% and 0.04% of MMC for 2 min. No MMC treatments were used as controls. Once 90% confluence was reached, cells were trypsinized and mixed with equal amounts of 0.4% trypan blue solution. Dead cells (e.g. with ruptured membranes) stained blue and live cells white and were counted using automated cell counter. Cellular viability was calculated as a percent.

A fluorescence-based TUNEL assay was used to detect DNA fragmentation and apoptosis in CSFs. The 0.02% dose of MMC treated and untreated CSFs were fixed in acetone at −20 °C for 2 min, dried at room temperature for 5 min, and placed in PBS balanced salt solution. Apoptosis was detected with ApopTag apoptosis detection kit (Millipore, Billerica, MA, USA) following manufacturer's instructions. Photographs were obtained using a fluorescent microscope (Leica) equipped with a digital camera (SpotCam RT KE; Diagnostic Instruments Inc., Sterling Heights, MI, USA).

Immunocytochemical analyses and quantification of anti-fibrotic effect of MMC

Immunofluorescent studies were carried out for αSMA (a myofibroblast marker) and F-actin. Immunostaining was performed using mouse monoclonal antibody for αSMA. The myofibroblast formation in CSF cultures was stimulated with TGFβ1. To evaluate anti-fibrotic effect of MMC, 0.02% MMC was added to cultures for 2 min, 11 days after TGFβ1 stimulation. A single 0.02% MMC treatment for 2 min demonstrated least toxicity to CSFs. At study endpoint (11 days), the cells were fixed with 4% paraformaldehyde, followed by

blocking with 5% BSA. The cells were then incubated at room temperature with mouse monoclonal antibody for αSMA (DAKO, Carpinteria, CA, USA) at a 1:500 dilution in 1· PBS for 90 min and with secondary antibody Alexa Fluor 488 goat anti-mouse IgG (Invitrogen) at a dilution of 1:1000 for 1 h. Cells were mounted with Vectashield containing 4′, 6-diamidino-2-phenylindole (DAPI) (Vector Laboratories, Inc., Burlingame, CA, USA) to allow visualization of nuclei. For F-actin, Alexa Fluor 594 anti-Phalloidin marker was used. The protocol provided by Molecular Probes (Invitrogen) was followed.

Tissue culture plates were examined and photographed with a Leica fluorescent microscope (Leica) equipped with a digital camera (SpotCam RT KE; Diagnostic Instruments Inc) at the conclusion of the study. The αSMA and DAPI-stained cells in ten randomly selected areas were counted per 100· and/or 200· microscope field.

Immunoblotting

Canine stromal fibroblasts were washed with ice-cold PBS and lysed in radio immunoprecipitation assay lysis buffer (Santa Cruz Biotechnology, Santa Cruz, CA, USA) containing protease inhibitor cocktail (Roche Applied Sciences, Indianapolis, IN, USA). The samples were suspended in Laemmli's denaturing sample buffer (30 μL) containing β-mercaptoethanol, vortexed for 1 min, centrifuged for 5 min at 10 000 *g*, and boiled at 90 °C for 5 min. Protein samples were resolved by 4–10% SDS–PAGE and transferred to a 0.45-μm pore size PVDF membrane (Invitrogen, San Diego, CA, USA). The membrane was incubated with αSMA (DAKO) (1:500 dilution in 5% nonfat dry milk) or β-actin primary antibodies (Santa Cruz Biotechnology Inc) (1:500 dilution) followed by AP-conjugated secondary anti-mouse antibodies (Santa Cruz Biotechnology Inc) (1:1000 dilution).

RNA extraction, cDNA synthesis and quantitative real-time PCR

The total RNA from CSF cultures (11 days) was extracted using RNeasy kit (Qiagen Inc., Valencia, CA, USA) and reverse-transcribed to cDNA following manufacturer's instructions (Promega, Madison, WI, USA). Real-time PCR was performed using iQ5 real-time PCR Detection System (Bio-Rad Laboratories, Hercules, CA, USA). A 20-μL reaction mixture containing 2 μL cDNA, 2 μL forward (200 nM), 2 μL reverse primer (200 nM), and 10 μL 2· iQ SYBR green super mix (Bio-Rad Laboratories) was run at universal cycle (95 °C for 3 min, 40 cycles of 95 °C for 30 s followed by 60 °C for 60 s) following manufacturer's instructions. For αSMA, forward primer sequence TGGGTGACGAAGCACAGAGC and reverse primer sequence CTTCAGGGGCAACACGAAGC were used. The house-keeping gene beta-actin forward primer sequence was CGGCTACAGCTTCACCACCA and reverse primer sequence was CGGGCAGCTCGTAGCTCTTC. The threshold cycle (C_T) was used to detect the increase in the signal associated with an exponential growth of PCR product during the log-linear phase. The relative gene expression was calculated using the following formula: $2^{-\Delta\Delta C_T}$. The C_T is a PCR cycle number at which the fluorescence meets the threshold in the amplification plot and DC_T is a subtraction product of target and housekeeping genes C_T values. The $2^{-\Delta\Delta C_T}$ is a method for determining relative target mRNA quantity in samples. The amplification efficiency for all used templates was validated by ensuring that the difference between linear slopes for all templates <0.1. Three independent reactions were performed and the average (± standard error of the mean or SEM) results were calculated.

Quantification and statistical analysis

The immunocytochemistry data quantification was performed by counting SMA-, F-actin-, TUNEL- and DAPI-positive colored cells in six randomly selected nonoverlapping areas of fluorescent cultures at 100· and 200· magnification field under Leica fluorescent microscope (Leica). The results were expressed as mean ± SEM. Statistical analysis of quantitative PCR

was performed with one-way analysis of variance (ANOVA) followed by Tukey's multiple comparison tests, and immunocytochemistry by Student's *t*-test. A *P*-value <0.05 was considered significant. Quantification of immunoblotting data was performed with I_{MAGE} J 1.38 X analysis software (NIH, Bethesda, MD, USA).

RESULTS

Cellular morphology and viability

To determine the potential toxicity of MMC, CSFs were treated with three different concentrations (0.002%, 0.02%, and 0.04%) of MMC. Cellular morphology was observed under phase-contrast microscope (Fig. 1). Panel a (untreated control), panel b (0.002% MMC) and panel c (0.02% MMC) showed no change in cellular morphology. However, a higher dose of 0.04% (panel d) significantly decreased the percentage of cellular viability (Figs 1,2). Percentage of cellular viability was demonstrated by trypan blue assay. Viable cells were counted by using automated cell counter and percentage of viability was estimated. A gradual decrease in the percentage of viable cells (5–27%) with increased dosage of MMC was found (Fig. 2). The reduction in the percentage of viable cells compared to untreated control was not statistically significant at 0.02% MMC; however, 0.04% MMC significantly reduced the percentage of viable cells up to 27% ($P < 0.001$) compared to the untreated control and compared to the 0.02% MMC dose ($P < 0.001$).

Apoptosis with TUNEL assay

We further evaluated the cytotoxicity of MMC on canine fibroblast and myofibroblast cell types by measuring cell death with TUNEL assay. Canine corneal fibroblasts (Fig. 3a,b) as well as TGFβ-induced myofibroblasts (Fig. 3c,d) were exposed to 0.02% MMC for 2 min (panels b and d). As shown in Fig. 3, the untreated controls (panels a and c) demonstrated 1–4 TUNEL-positive cells (red) whereas MMC-treated cultures (panels b and d) showed 3–8 TUNEL-positive red cells.

F-actin immunocytochemistry

Cytoskeletal changes and contractions are an integral component of normal wound healing and tissue remodeling. The effects of MMC treatment on the cytoskeletal components of canine corneal fibroblasts and myofibroblasts were examined by measuring expression of F-actin immunostaining (Fig. 4).MMC 0.02% treated canine corneal fibroblasts (panel b) and TGFβ-induced canine corneal myofibroblasts (panel d) showed significant reduction in F-actin levels compared to the MMC untreated controls (panels a and c). Digital quantification of three independent experiments (3-wells for each treatment) found 51–59% ($P < 0.01$) reduction in number of F-actin positive cells in MMC-treated cultures (figure not shown).

αSMA immunocytochemistry, quantification and immunoblotting

The effect of 0.02% MMC on canine fibrosis was analyzed by measuring the levels of αSMA (a fibrosis marker) in CSF and TGFβ-induced myofibroblast cultures. The immunocytochemistry results of cultures prepared in the presence or absence of 0.02% MMC are demonstrated in Fig. 5. Untreated control corneal fibroblasts (panel a) showed marginal expression of αSMA that was significantly decreased with MMC treatment (panel b) (92–97%, $P < 0.001$). TGFβ successfully differentiated CSF to myofibroblasts (panel c), as evidenced by significant high levels of αSMA (84–93%, $P < 0.001$). The MMC treatment (panel d) showed significant inhibition of TGFβ-induced myofibroblast and αSMA development (59–67%, $P < 0.001$) compared to the MMC-untreated control (panel c). The quantification of αSMA immunocytochemical data has been summarized in Fig. 6. DAPI-

stained nuclei of αSMA positive cells were counted at 100· magnification in six nonoverlapping areas.

Results of αSMA protein quantification using Western blot analysis are shown in Fig. 7. Canine corneal myofibroblast cultures grown under serum-free conditions in presence of TGFβ (1 ng/mL) were either treated with 0.02% MMC or left untreated. Untreated controls were likewise grown under serum-free conditions but did not receive TGFβ or MMC treatment. Level of αSMA protein expression in myofibroblasts treated with TGFβ significantly increased compared to the untreated controls (10-fold, Fig. 7, lane 2). Treatment of 0.02% MMC in presence of TGFβ reduced the level of αSMA expression significantly ($P < 0.01$) (Fig. 7, lane 3). Beta-actin was used as a loading control. The immunoblotting data was quantified with NIH image analysis software. The analysis of data after normalization further confirmed the anti-fibrotic effect of MMC on CSFs is significant ($P < 0.01$).

αSMA RNA quantification

Figure 8 shows quantification of αSMA RNA performed with real-time PCR. A statistically significant 10-fold increase in αSMA RNA was detected in CSFs exposed to TGFβ only compared to the untreated control ($P < 0.01$). Application of 0.02% MMC in presence of TGFβ demonstrated highly significant eightfold reduction of αSMA RNA ($P < 0.001$). Beta-actin was used as the house-keeping control.

DISCUSSION

Corneal injury from any cause immediately activates the process of corneal wound healing.[23,24] This process has been studied prolifically with the inception of surface ablation procedures in physician ophthalmology. Both deep epithelization as well as laser-mediated ablation induces keratocyte apoptosis.[25] This is followed by proliferation and migration of the surrounding keratocytes to repopulate the denuded stroma.[26] In response to endogenous epithelial derived cytokines, especially TGFβ,[27] a population of keratocytes transdifferentiate into myofibroblasts. This population of cells participates in cellular matrix remodeling, resulting in a more disorganized extracellular matrix, with abundant collagen type III and IV populations that contributes to loss of corneal transparency.[3–6] This mechanism eventually leads to the formation of corneal fibrosis.[3] Myofibroblasts are contractile and metabolically active opaque cells that contain intracellular microfilament bundles of F-actin and αSMA.[7,23] They are critical to normal corneal wound healing and once this process is complete the population of myofibroblasts decreases due to apoptosis.[6,23,27] Multiple studies have shown that a decrease in myofibroblast production significantly reduces corneal fibrosis or haze.[13,23,28,29]

Presently, MMC has been extensively used clinically by physician ophthalmologists to prevent corneal haze. It significantly inhibits proliferation of corneal epithelial, stromal and endothelial cells, conjunctival fibroblasts and retinal pigment epithelial cells.[13,30–34] It is a genotoxic antibiotic first isolated from cultures of *Streptomyces caespitosus* by Hata in 1956.[35,36] Upon activation by enzymes such as cytochrome p450 reductase, it cross-links DNA molecules between adenine and guanine and thereby blocks DNA synthesis, eventually causing cell cycle arrest.[17,37–41] Due to its anti-mitotic effect, cells with higher mitotic rate are more sensitive to its action, hence MMC is widely used as a chemotherapeutic agent.[42] It has been extensively used for treatment of corneal scarring in various species including rodents, rabbits, as well as humans both *in vivo* and *in vitro*. Our laboratory has recently published the effects of MMC on equine corneal fibroblasts in an *in vitro* model.[20] The purpose of our study was to elucidate the toxic and anti-fibrotic effects of MMC on cultured CSFs. We investigated the safety and therapeutic efficiency of MMC on

fibroblasts as well as myofibroblasts using an *in vitro* model of canine corneal fibrosis. The 0.02% dose of MMC that is currently frequently used by many physician ophthalmologists postoperatively during ocular surgery did not alter the morphology of CSFs. However, TUNEL assays demonstrated an increase in number of apoptotic cells as well as decrease in cellular viability at higher concentrations of MMC (0.04%). Significant suppression of myofibroblast formation by MMC was demonstrated using immunocytochemical analysis for F-actin and antifibrotic αSMA. Moreover, real-time PCR analysis also confirmed the reduction in expression of αSMA in MMC treated cells. These findings are consistent with our *in vitro* human and equine as well as *in vivo* rabbit studies that showed reduction in corneal scarring with MMC was due to increased apoptosis and decreased cellular proliferation. [14] This study's results suggest that MMC may have promising potential for the treatment of corneal fibrosis in clinical canine patients, improving their long-term visual outcome.

Although effectiveness of MMC in treatment of corneal fibrosis has been well-established in various species, contradictory studies regarding its safety in people are reported. Due to safety concerns, different protocols stating different concentrations and exposure times have been reported and used by clinicians to minimize unwanted side effects of MMC.[9] In this study, we have addressed the safety of MMC on canine corneal keratocytes using an *in vitro* model. We evaluated CSF morphology, proliferation and cell death in response to various concentrations of MMC using various biochemical techniques. Notably, corneal epithelial cell toxicity was not evaluated in this study and should be considered in future *in vitro* and *in vivo* studies. The range of MMC concentrations used in this investigation revealed that a 0.02%dose with an exposure time of 2 min did not alter cellular morphology or phenotype and would therefore be a reasonable starting dose for future canine *in vivo* investigations. Further studies are warranted to determine optimal dosage of MMC for treatment of corneal fibrosis in clinical patients.

Acknowledgments

Funding for this project was provided through the RO1EY017294 (RRM) grant from the National Eye Institute, National Institutes of Health, Bethesda, MD, USA and an unrestricted grant from the Research to Prevent Blindness, New York, NY, USA.

REFERENCES

1. Hu C, Ding Y, Chen J, et al. Basic fibroblast growth factor stimulates epithelial cell growth and epithelial wound healing in canine corneas. Veterinary Ophthalmology. 2009; 12:170–175. [PubMed: 19392876]
2. Chang SW, Chou SF, Chuang JL. Mechanical corneal epithelium scraping and ethanol treatment up-regulate cytokine gene expression differently in rabbit cornea. Journal of Refractive Surgery. 2008; 24:150–159. [PubMed: 18297939]
3. Saika S. TGF beta pathobiology in the eye. Laboratory Investigation. 2006; 86:106–115. [PubMed: 16341020]
4. Dawson DG, Edelhauser HF, Grossniklaus HE. Long-term histopathologic findings in human corneal wounds after refractive surgical procedures. American Journal of Ophthalmology. 2005; 139:168–178. [PubMed: 15652843]
5. Moller-Pedersen T, Cavanagh HD, Petroll WM, et al. Stromal wound healing explains refractive instability and haze development after photorefractive keratectomy. A 1-year confocal microscopy study. Ophthalmology. 2000; 107:1235–1245. [PubMed: 10889092]
6. Moller-Pedersen T. Keratocyte reflectivity and corneal haze. Experimental Eye Research. 2004; 78:553–560. [PubMed: 15106935]
7. Jester JV, Petroll WM, Cavanagh HD. Corneal stromal wound healing in refractive surgery: the role of myofibroblasts. Progress in Retinal and Eye Research. 1999; 18:311–356. [PubMed: 10192516]

8. Meeke KM, Boote C. The organization of collagen in corneal stroma. Experimental Eye Research. 2004; 78:503–512. [PubMed: 15106929]
9. Song JS, Kim JH, Yang M, et al. Mitomycin C concentration in the cornea and aqueous humor and apoptosis in the stroma after topical mitomycin C application. Effects of mitomycin C application time and concentration. Cornea. 2007; 26:461–467. [PubMed: 17457196]
10. Abraham LM, Selva D, Casson R, et al. Mitomycin: clinical application in ophthalmic practice. Drugs. 2006; 66:321–340. [PubMed: 16526821]
11. Gambato C, Ghirlando A, Moretto E, et al. Mitomycin C modulation of corneal wound healing after photorefractive keratectomy in highly myopic eyes. Ophthalmology. 2005; 112:208–218. [PubMed: 15691552]
12. Thornton I, Xu M, Krueger RR. Comparison of standard (0.02%) and low dose (0.002%) mitomycin C in the prevention of corneal haze following surface ablation for myopia. Journal of Refractive Surgery. 2008; 24:S68–S76. [PubMed: 18269154]
13. Chang SW. Early corneal edema following topical application of mitomycin C. Journal of Cataract and Refractive Surgery. 2004; 30:1742–1750. [PubMed: 15313301]
14. Netto MV, Mohan RR, Sinha S, et al. Effect of prophylactic and therapeutic mitomycin C on corneal apoptosis, cellular proliferation, haze and long term keratocyte density in rabbits. Journal of Refractive Surgery. 2006; 22:562–574. [PubMed: 16805119]
15. Chang SW. Corneal keratocyte apoptosis following topical intra-operative mitomycin C in rabbits. Journal of Refractive Surgery. 2005; 21:446–453. [PubMed: 16209441]
16. Kim TI, Tchah H, Lee SA, et al. Apoptosis in keratocytes caused by mitomycin C. Investigative Ophthalmology and Visual Science. 2003; 44:1912–1917. [PubMed: 12714623]
17. Chou SF, Chang SW, Chuang JL. Mitomycin C up-regulates IL-8y MCP-1 chemokine expression via mitogen activated protein kinases in corneal fibroblasts. Investigative Ophthalmology and Visual Science. 2007; 48:2009–2016. [PubMed: 17460254]
18. Crowston JG, Chang LH, Constable PH, et al. Apoptosis gene expression and death receptor signaling in mitomycin C treated human tenon capsule fibroblasts. Investigative Ophthalmology and Visual Science. 2002; 43:692–699. [PubMed: 11867586]
19. Seong GJ, Park C, Kim CY, et al. Mitomycin C induces apoptosis of human Tenon's capsule fibroblasts by activation of c-Jun N-terminal kinase 1 and caspase-3 protease. Investigative Ophthalmology and Visual Science. 2005; 46:3545–3552. [PubMed: 16186332]
20. Buss D, Sharma A, Giuliano EA, et al. Efficacy and safety of mitomycin C as an agent to treat corneal scarring in horses using an *in vitro* model. Veterinary Ophthalmology. 2010; 13:211–218. [PubMed: 20618797]
21. Karasawa K, Matsuda H, Tanaka A. Superficial keratectomy and topical mitomycin C as therapy for corneal squamous cell carcinoma in a dog. Journal of Small Animal Practice. 2008; 4:208–210. [PubMed: 17725585]
22. Glover TL, Nasisse MP, Davidson MG. Effects of topically applied mitomycin C on intraocular pressure, facility of outflow, and fibrosis after glaucoma filtration surgery in clinically normal dogs. American Journal of Veterinary Research. 1995; 7:936–940. [PubMed: 7574164]
23. Boote C, Dennis S, Newton RH, et al. Collagen fibrils appear more closely packed in the prepupillary cornea: optical and biomechanical implications. Investigative Ophthalmology and Visual Science. 2003; 44:2941–2948. [PubMed: 12824235]
24. Wilson SE, Mohan RR, Ambrosio R Jr, et al. The corneal wound healing response: cytokine-mediated interaction of epithelium, stroma and inflammatory cells. Progress in Retinal Eye Research. 2001; 20:625–637.
25. Dupps WJ, Wilson SE. Biomechanics and wound healing in the cornea. Experimental Eye Research. 2006; 83:709–720. [PubMed: 16720023]
26. Rajan MS, O'Brart DPS, Patmore A, et al. Cellular effects of mitomycin C on human corneas after photorefractive keratectomy. Journal of Cataract and Refractive Surgery. 2006; 32:1741–1747. [PubMed: 17010877]
27. Jester JV, Ho-Chang J. Modulation of cultured corneal keratocyte phenotype by growth factors/cytokines control *in vitro* contractility and extracellular matrix contraction. Experimental Eye Research. 2003; 77:581–592. [PubMed: 14550400]

28. Conrad GW, Funderburgh JL. Eye development and appearance and maintenance of corneal transparency. Transactions of the Kansas Academy of Science. 1992; 95:34–38. [PubMed: 11537981]
29. Maurice DM. The transparency of the corneal stroma. Vision Research. 1970; 10:107–108. [PubMed: 5435007]
30. Netto MV, Mohan RR, Ambrosio R Jr. Wound healing in the cornea: a review of refractive surgery complications and new prospects for therapy. Cornea. 2005; 24:509–522. [PubMed: 15968154]
31. Nuyts RM, Pels E, Greve EL. The effects of 5-fluorouracil and mitomycin C on the corneal endothelium. Current Eye Research. 1992; 11:565–570. [PubMed: 1505200]
32. Jampel HD. Effect of brief exposure to mitomycin C on viability and proliferation of cultured human Tenon's capsule fibroblasts. Ophthalmology. 1992; 99:1471–1476. [PubMed: 1407982]
33. Kang SG, Chung H, Yoo YD, et al. Mechanism of growth inhibitory effect of mitomycin C on cultured human retinal pigment epithelial cells: apoptosis and cell cycle arrest. Current Eye Research. 2001; 22:174–181. [PubMed: 11462153]
34. Wu KY, Hong SJ, Huang HT, et al. Toxic effects of mitomycin C on cultured corneal keratocytes and endothelial cells. Journal of Ocular Pharmacology and Therapeutics. 1999; 15:401–411. [PubMed: 10530701]
35. Chabner, BA.; Ryan, DP.; Paz-Ares, L., et al. Antineoplastic agents. In: Hardman, JG.; Limbrid, LE.; Goodman, Gilman A., editors. The Pharmacological Basis of Therapeutics. 10th edn.. New York: McGraw Hill; 2001. p. 1389-1459.
36. Skolnick, AC.; Grimmett, MR. Management of pterigium. In: Krachmer, JH.; Mannis, MJ.; Holland, EJ., editors. Cornea. 2nd edn.. Philadelphia, PA: Elsevier Mosby; 2005. p. 1873-1892.
37. Bligh HF, Bartoszek A, Robson CN, et al. Activation of mitomycin C by NADPH:cytochrome p-450 reductase. Cancer Research. 1990; 50:7789–7792. [PubMed: 2123741]
38. Cummings J, Spanswick VJ, Tomasz M, et al. Enzymology of mitomycin C metabolic activation in tumor tissue: implications for enzyme-directed bioreductive drug development. Biochemical Pharmacology. 1998; 56:405–414. [PubMed: 9763215]
39. Wang SL, Han JF, He XY, et al. Genetic variation of human cytochrome p-450 reductase as a potential biomarker for mitomycin C induced cytotoxicity. Drug Metabolism and Disposition. 2007; 35:176–179. [PubMed: 17062779]
40. Isliah M, Halstead BW, Kadura IA, et al. Relationships between genomic, cell cycle, and mutagenic responses of TK6 cells exposed to DNA damaging chemicals. Mutation Research. 2005; 578:100–116. [PubMed: 16109433]
41. Mladenov E, Tsaneva I, Anachkova B. Activation of the S phase DNA damage checkpoint by mitomycin C. Journal of Cellular Physiology. 2007; 211:468–476. [PubMed: 17167777]
42. Verweij J, Pinedo HM. Mitomycin C: mechanism of action, usefulness and limitations. Anti-Cancer Drugs. 1990; 1:5–13. [PubMed: 2131038]

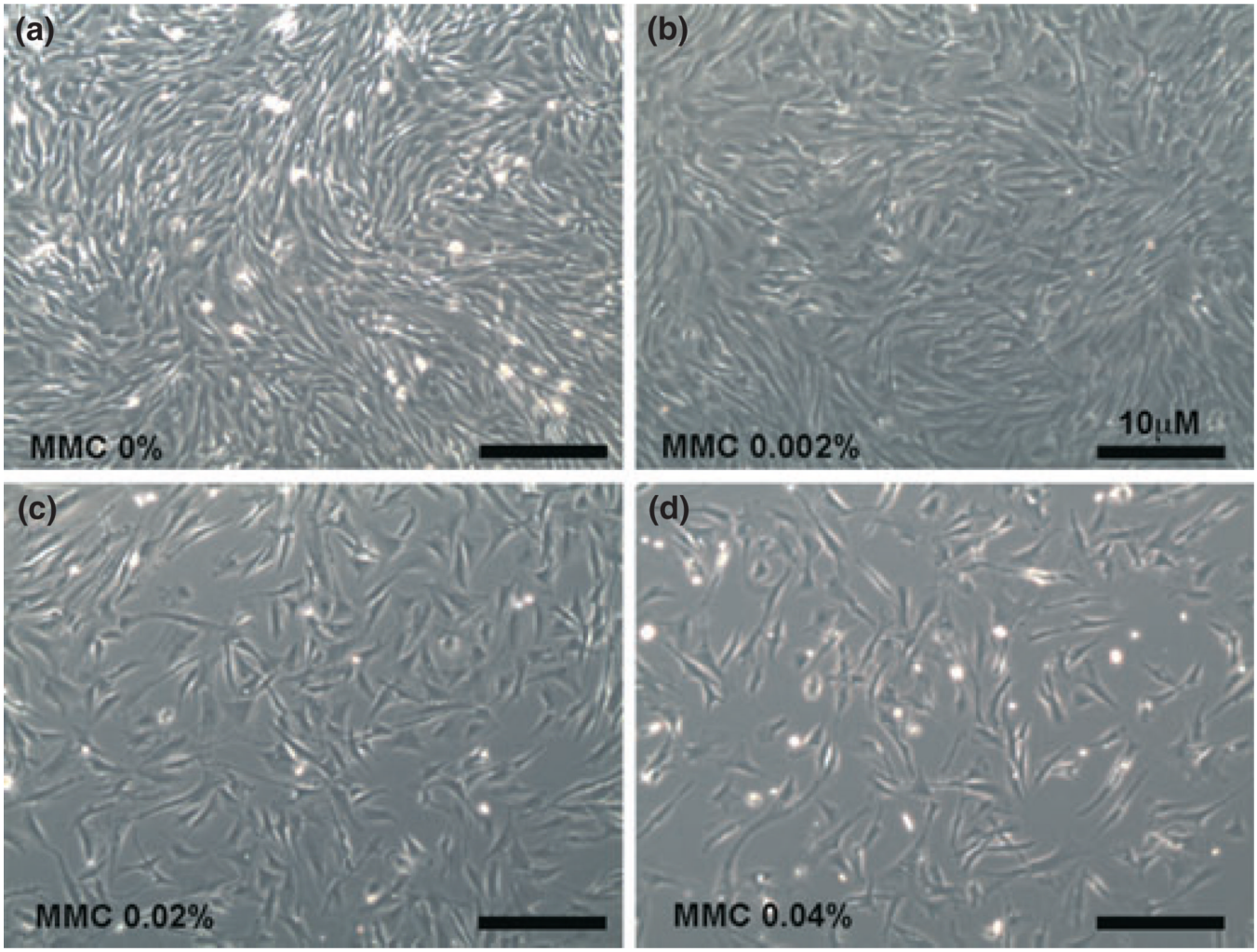

Figure 1.

Dose-dependent treatment of mitomycin C (MMC) in canine stromal fibroblast (CSF) primary cultures. Bright-field images of CSF cultures were taken using a light microscope. (a) Untreated control and (b) 0.002% MMC demonstrated no change in cellular morphology. A single 2 min dose of 0.02% MMC (c) did not alter cellular morphology. Higher doses of MMC (0.04%, d) reduced CSF populations considerably without altering phenotype or viability. The anti-fibrotic effects of MMC at low dose and short exposure times are likely due to proliferation or growth inhibition.

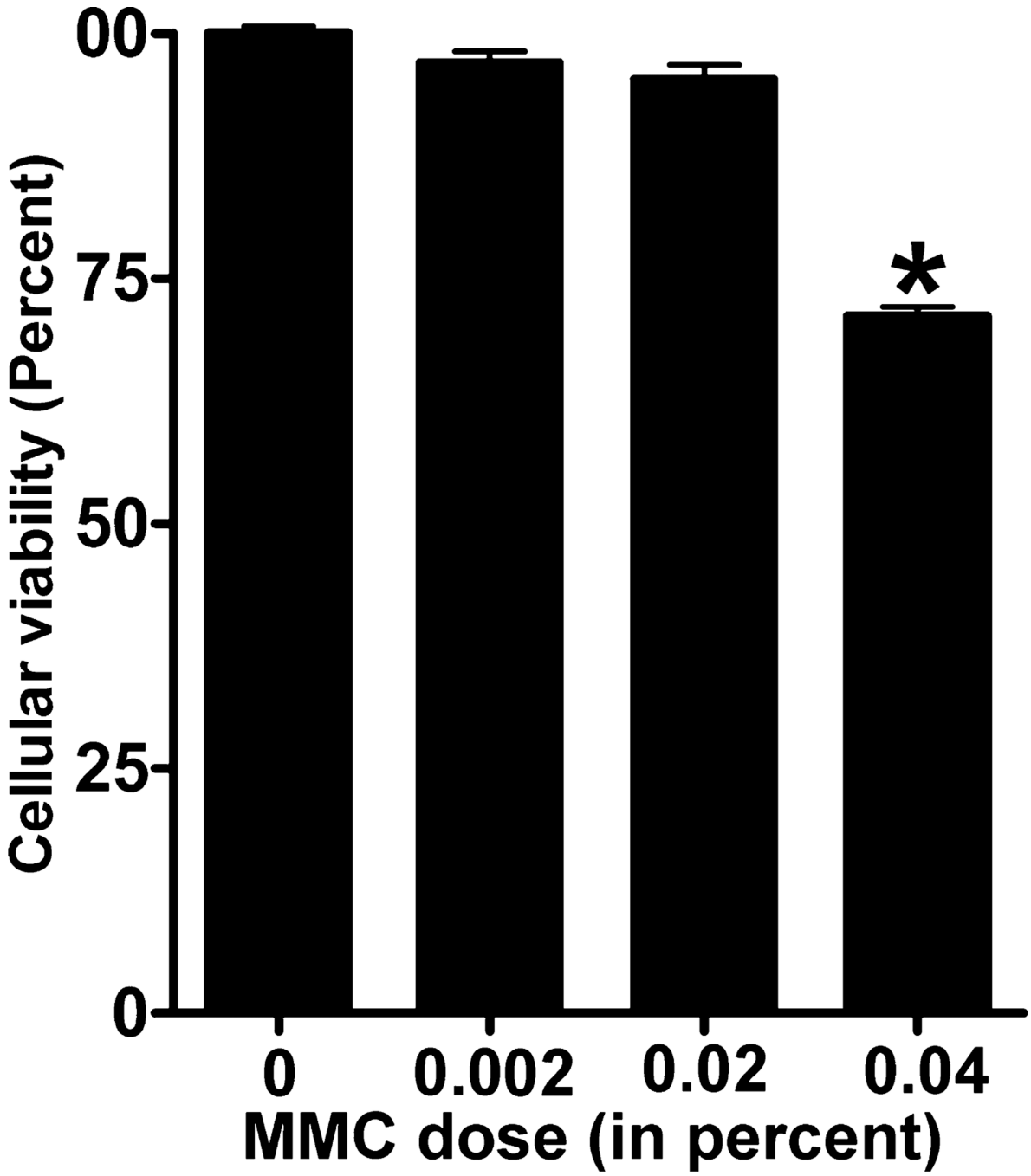

Figure 2.
Percent viability of canine stromal fibroblasts (CSFs) treated with increasing doses of mitomycin C (MMC). CSFs treated with various concentrations of MMC were stained with trypan blue reagent to count the number of viable cells. MMC dose of 0.002% and 0.02% only slightly decreased cellular viability but were not statistically significant. However, 0.04% significantly reduced the cellular viability up to 27% ($P < 0.001$). Error bars indicate standard error.

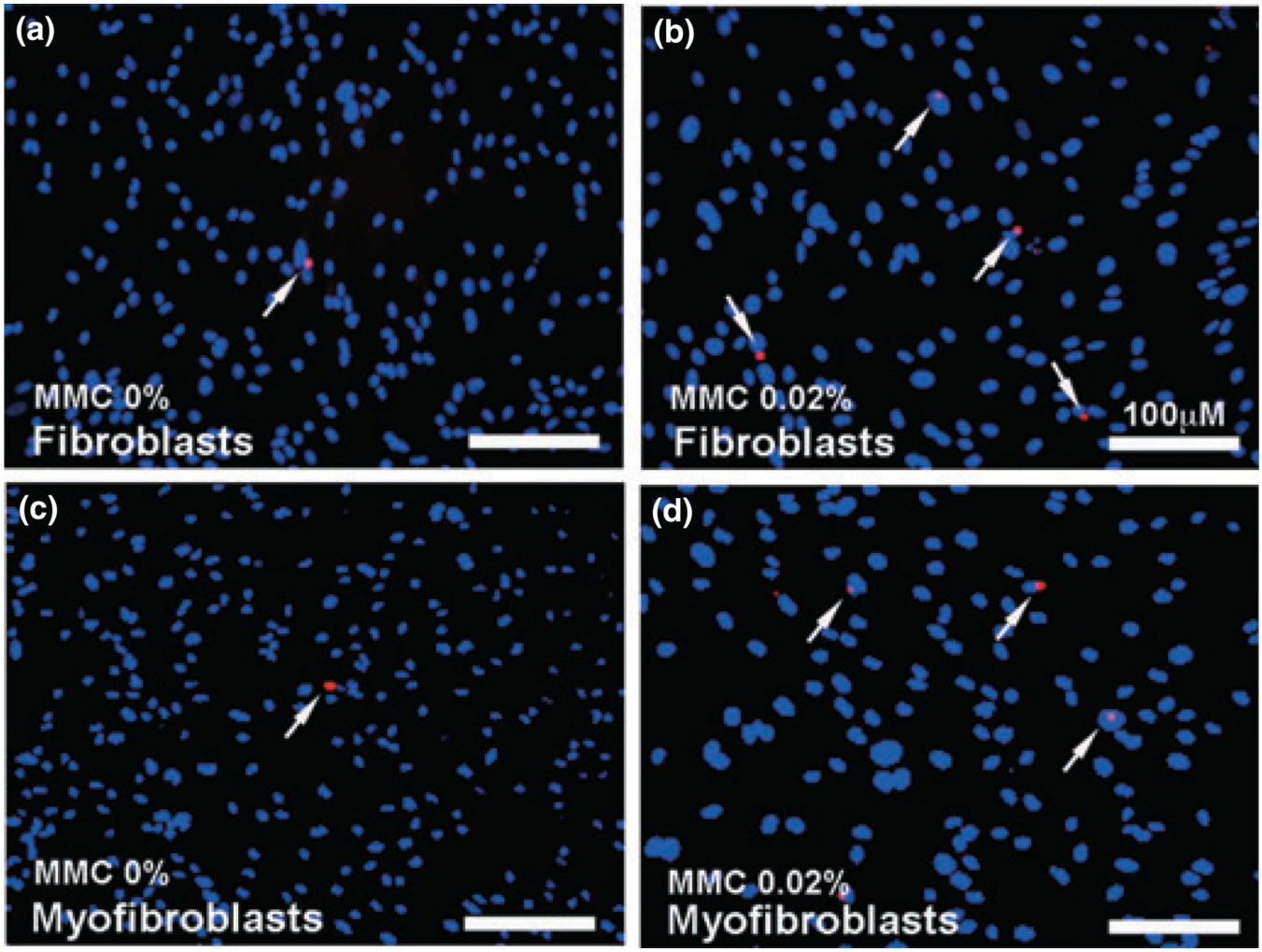

Figure 3.
Terminal deoxynucleotidyl transferase dUTP nick end labeling (TUNEL) assay demonstrating apoptotic cells in fibroblast and myofibroblast cultures treated with mitomycin C (MMC). Canine corneal fibroblasts (a, b) as well as TGFβ-induced myofibroblasts (c, d) were exposed to 0.02% MMC for 2 min. Based on six nonover-lapping fields quantification, MMC untreated controls (a, c) demonstrated 1–4 TUNEL-positive cells (red) whereas MMC-treated cultures (b, d) showed 3–8 TUNEL-positive red cells. The 0.02% MMC treatment for 2 min to canine corneal fibroblast and myofibroblast did not induce significant cell death. Arrows indicate apoptotic cells. Nuclei are stained blue with DAPI; scale bar denotes 100 μm.

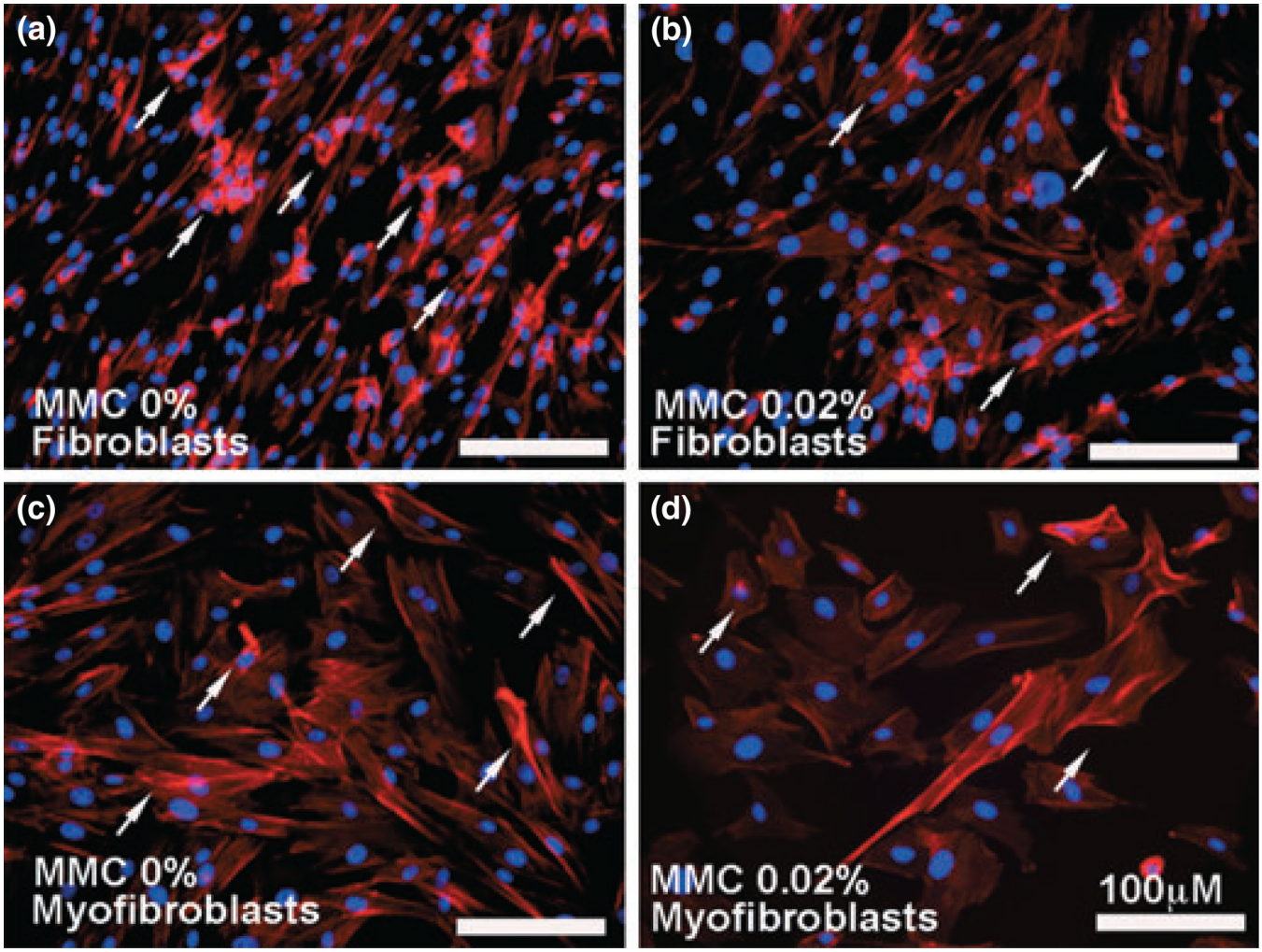

Figure 4.

Immunofluorescence studies demonstrating F-actin expression. Compared to the untreated controls (a, c), the 0.02% mitomycin C (MMC) treatment to canine corneal fibroblast (b) and myofibroblast cells (d) significantly reduced expression of F-actin (51–59%; $P < 0.01$) as per digital quantification. The arrows indicate F-actin positive cells. Nuclei are stained blue with DAPI; scale bar denotes 100 μm.

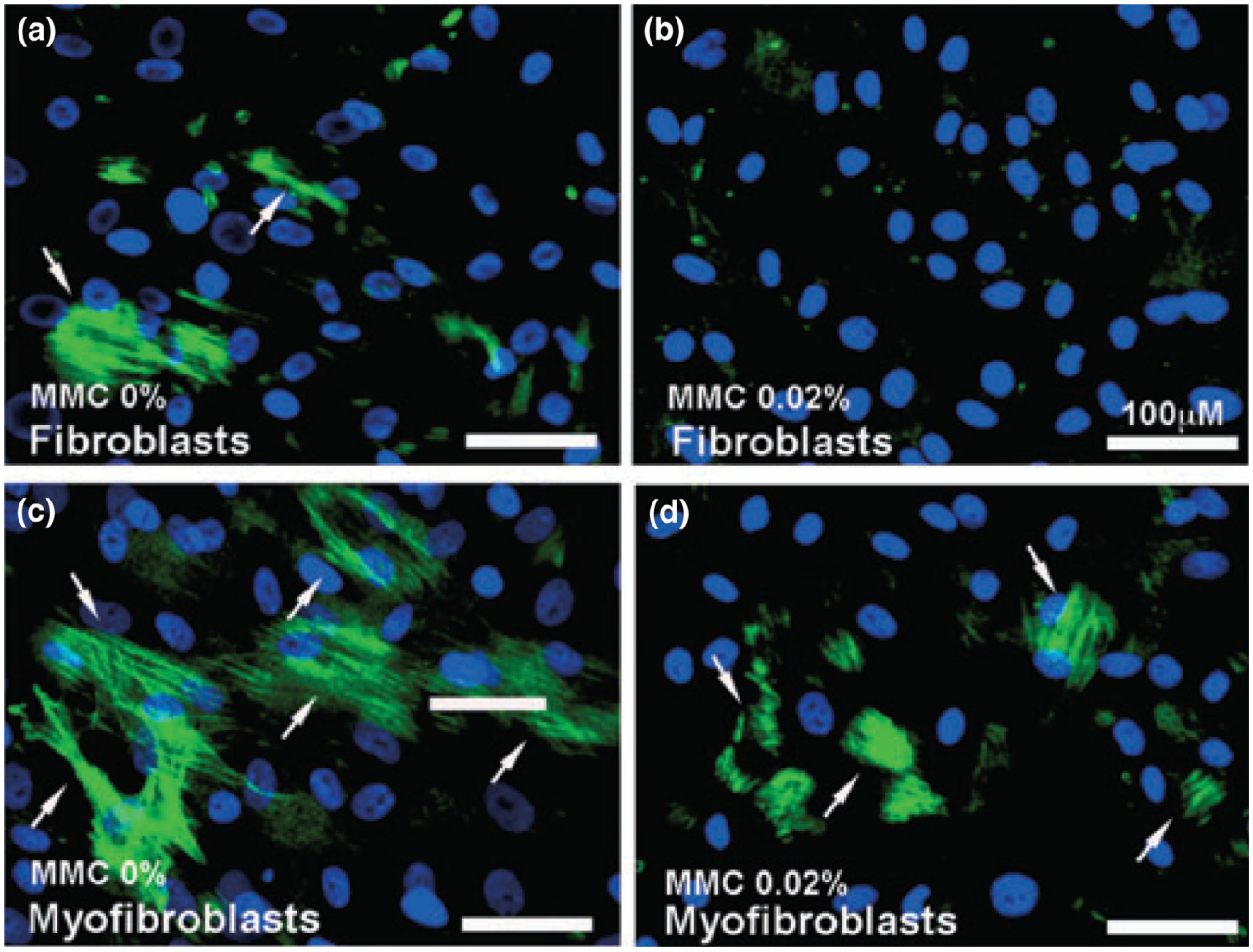

Figure 5.
Immunofluorescence studies demonstrating alpha smooth muscle actin (αSMA) expression in canine corneal cultures. The arrows indicate αSMA – positively stained cells (green). The 0.02% mitomycin C (MMC) treatment showed statistically significant reduction of αSMA in canine corneal fibroblast (b) and myofibroblast (d) compared to untreated controls (a, c). Nuclei are stained blue with DAPI; scale bar denotes 100 μm.

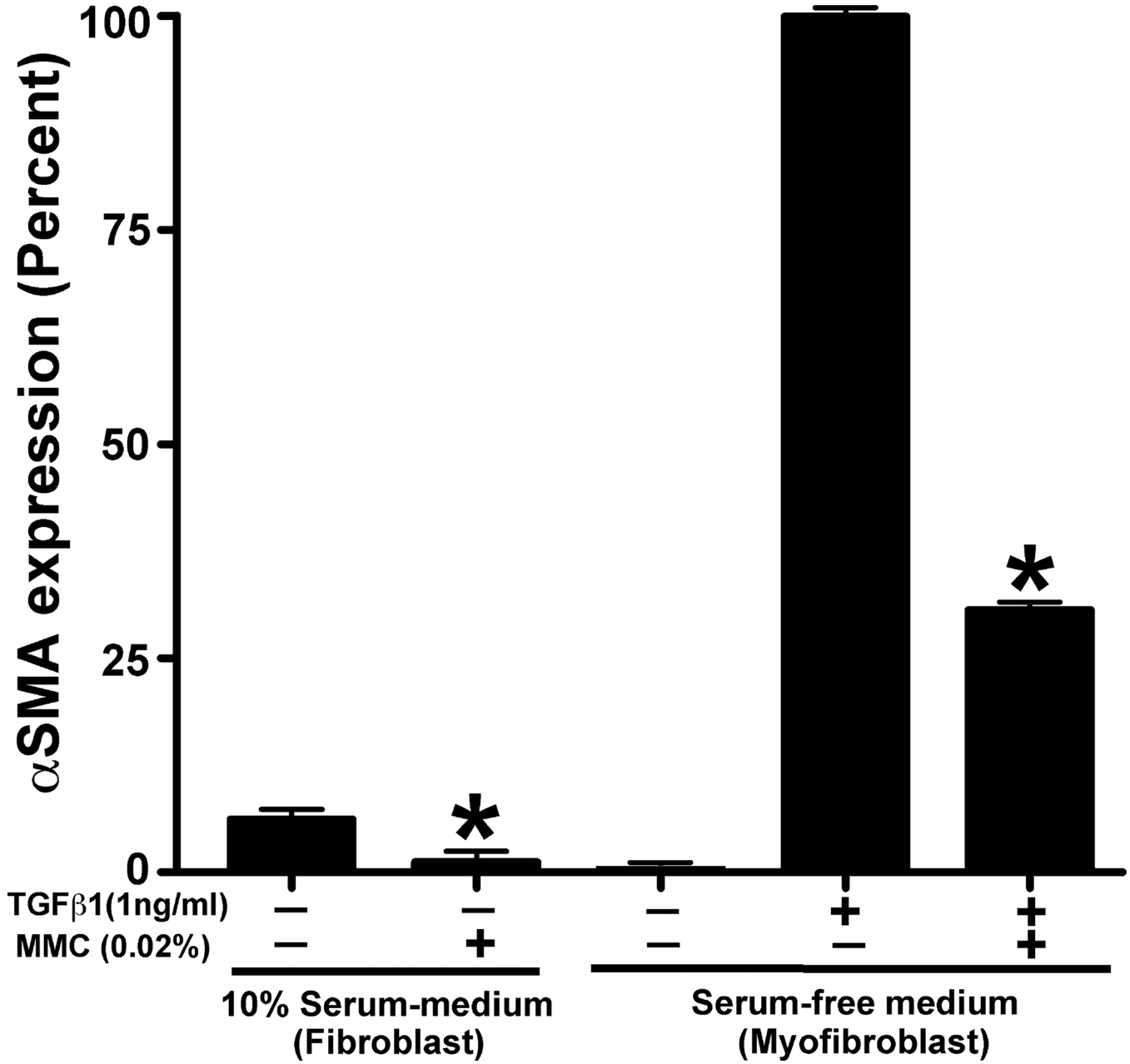

Figure 6.

Quantification of alpha smooth muscle actin (αSMA)-immunostained cells in canine stromal fibroblast (CSF) cultures treated with or without mitomycin C (MMC). The 0.02% MMC treatment showed statistically significant reduction of αSMA in CSF (grown in normal medium supplemented with 10% serum) (92–97%; $P < 0.001$) and myofibroblasts (grown in serum-free medium) (59–67%; $P < 0.001$) compared to untreated controls. Error bars indicate standard error.

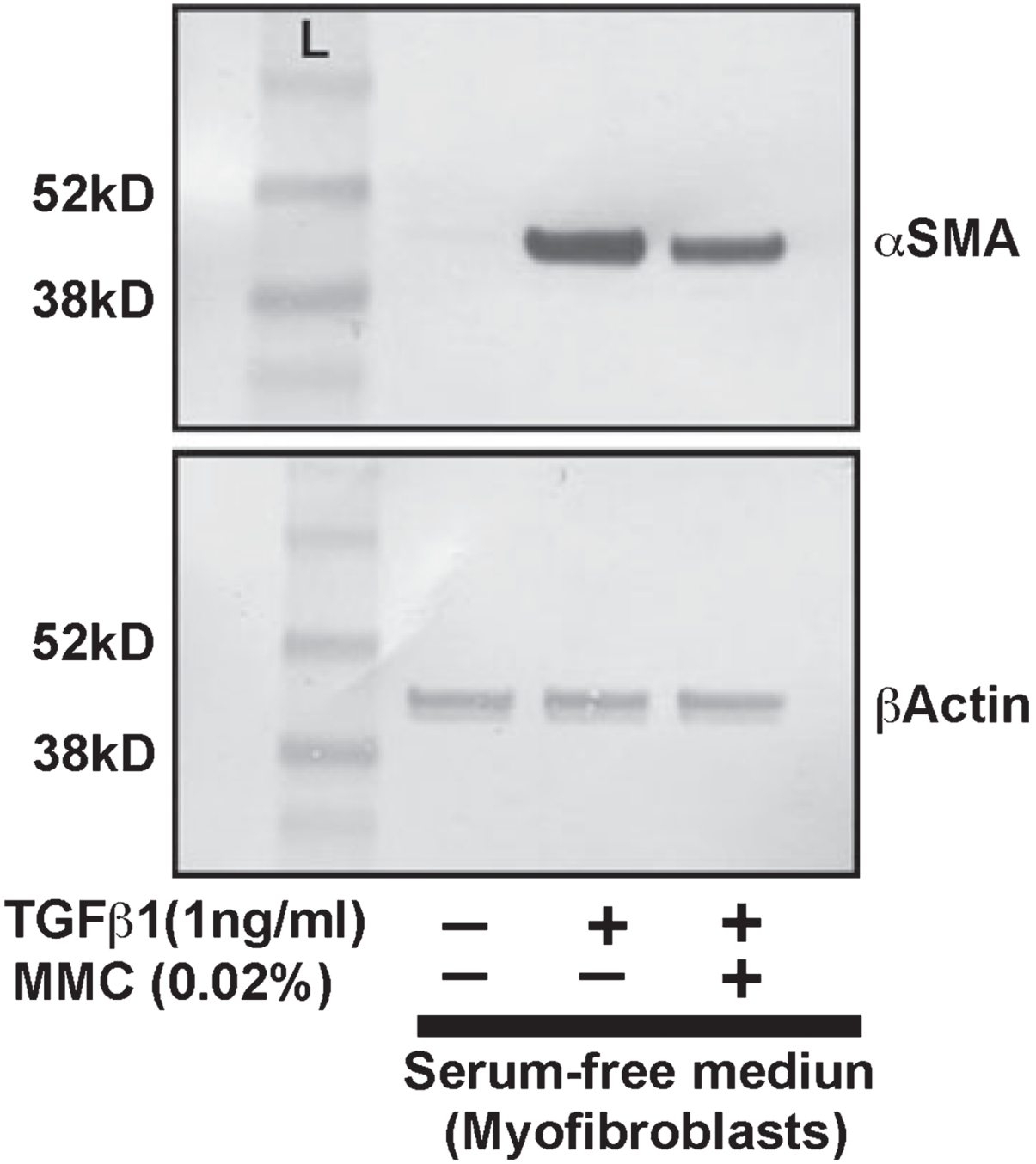

Figure 7.

Immunoblot analysis demonstrating quantitative measurement of alpha smooth muscle actin (αSMA) (myofibroblast marker) in canine stromal fibroblast (CSF) cultures treated with or without TGFβ1 and 0.02% mitomycin C (MMC). Equal quantity of protein (20 μg) was loaded in each lane. Lane 1 is the untreated control. Lysates prepared form TGFβ-treated cells were loaded in lane 2. TGFβ + MMC treated cell lysates were loaded in lane 3. Beta-actin was used as house keeping gene. A single MMC treatment (0.02% for 2 min) (lane 3) showed significant decrease in TGFβ1-induced myofibroblast formation (lane 2) in CSFs compared to untreated controls (lane 1).

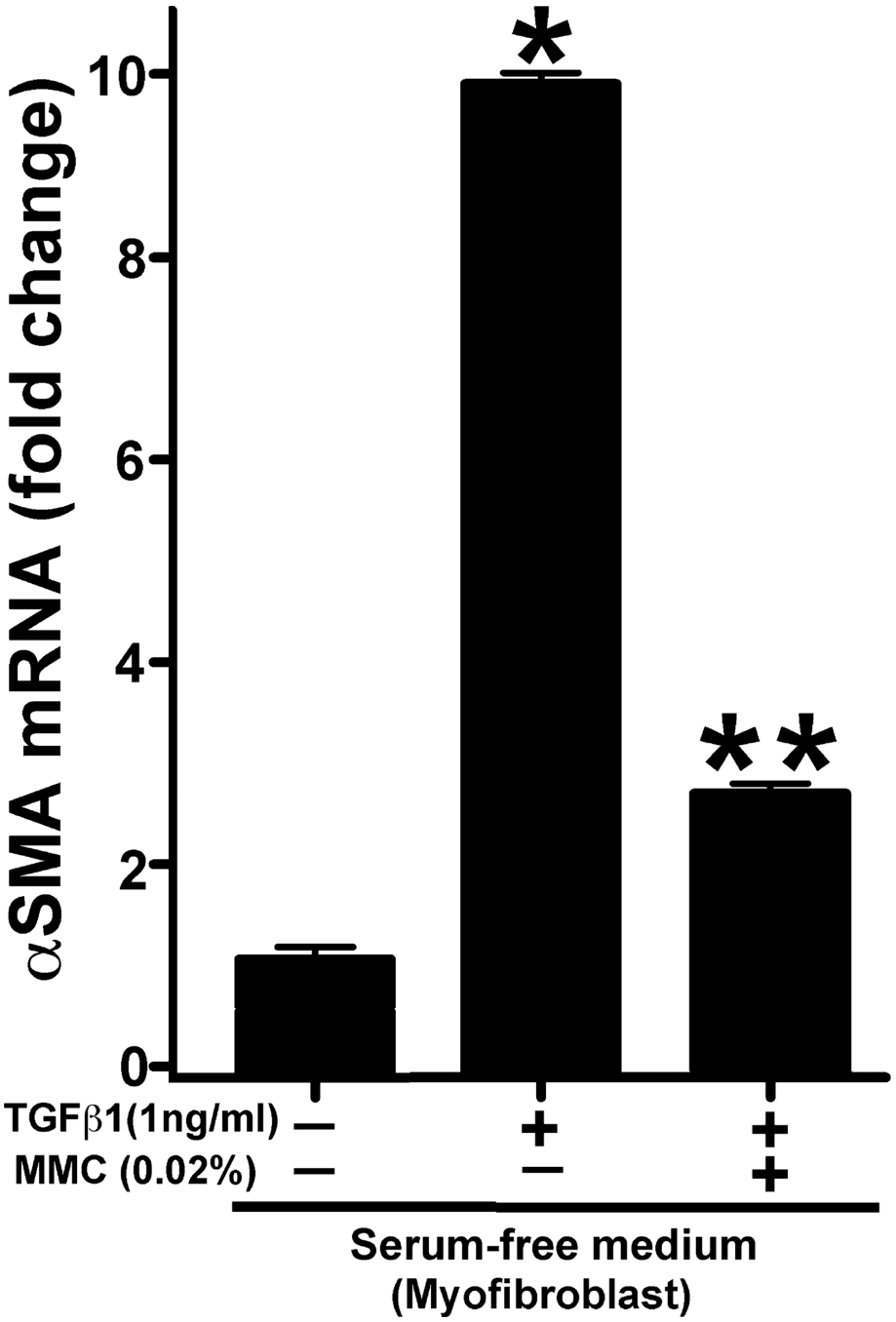

Figure 8.

Quantitative real-time PCR measurements of alpha smooth muscle actin (αSMA) in mitomycin C (MMC) treated or untreated myofibroblasts. TGFβ1 exposure induced significant αSMA formation (10-fold: $P < 0.01$) in myofibroblasts and 0.02% MMC treatment significantly decreased (eightfold: $P < 0.001$) TGFβ1-induced myofibroblast formation. Error bar indicates standard error.